ECCOMAS Congress 2016
VII European Congress on Computational Methods in Applied Sciences and Engineering
M. Papadrakakis, V. Papadopoulos, G. Stefanou, V. Plevris (eds.)
Crete Island, Greece, 5–10 June 2016

A PROBABILISTIC APPROACH TOWARDS AN EVALUATION OF EXISTING CODE PROVISIONS FOR SEISMICALLY ISOLATED STRUCTURES (ECCOMAS CONGRESS 2016)

Anastasios Tsiavos[1], **Bozidar Stojadinovic**[2]

[1] Doctoral Student, Institute of Structural Engineering, Swiss Federal Institute of Technology (ETH) Zürich, HIL E 12.1, Stefano-Franscini-Platz 5, 8093 Zürich, Switzerland
tsiavos@ibk.baug.ethz.ch

[2] Professor, Institute of Structural Engineering, Swiss Federal Institute of Technology (ETH) Zürich HIL E 14.1, Stefano-Franscini-Platz 5, 8093 Zurich, Switzerland
stojadinovic@ibk.baug.ethz.ch

Keywords: Seismic Isolation, Seismic probabilistic risk assessment, Performance-based design, Code provisions, Strength reduction factor

Abstract. *Following modern design codes, seismically isolated superstructures are designed to respond in the elastic response range or to exhibit limited inelastic behavior. However, the behavior of seismically isolated structures when the superstructure enters the inelastic response range has not been extensively investigated in the past. This paper aims at answering the following questions: What is the probability that a (code-compliant) seismically isolated structure will yield? Will it develop a ductility demand μ larger than that implied by its design strength reduction factor?*

The probabilistic investigation of such a behavior is important for two reasons: First, to estimate the conservativism implied by the existing code provisions for seismically isolated structures. Second, to account for the case in which the seismic forces acting on an existing seismically isolated structure could exceed the design forces due to a ground motion stronger than the design ground motion level. The investigation is conducted using a two-degree-of-freedom model of a seismically isolated structure. The hysteretic behavior of the seismic isolation devices and the isolated superstructure is simulated in Matlab and OpenSees using a bilinear elastic-plastic model. The results are obtained by analyzing the responses of the isolated structure to a large number of recorded ground motions.

Fragility curves to estimate the probability that the structure enters the inelastic range (μ>1), if it is designed according to the existing American and European code provisions for seismically isolated structures are determined through probabilistic seismic demand analysis (PSDA). The influence of the isolated structure overstrength and the isolation system hardening is discussed. Additional fragility curves are provided for other values of the engineering demand parameter (EDP) that are not allowed in the existing code provisions (e.g. superstructure displacement ductility μ>2). The effects of seismic isolation and superstructure design parameters on the fragility curves is quantified through parametric analysis.

1 INTRODUCTION

Base isolation is a seismic response modification technology developed in mid 1970's to control the extent of damage to structures subjected to strong ground motion excitation. However, the acceptance of the technology increased significantly after the observed response of seismically isolated structures in 3 earthquakes: The 1994 Northridge earthquake in the USA, the 1995 Hyogoken-Nanbu earthquake in Japan and the 1999 Chi-Chi earthquake in Taiwan. Over this period, the number of seismically isolated structures worldwide increased, and the building codes have been revised to include design requirements for seismically isolated structures [1].

The elastic design approach, which aims to avoid yielding of the isolated superstructure, is embedded in the design codes worldwide. Eurocode [2] allows a maximum behavior factor value of 1.5 for base-isolated buildings. US ASCE 7 [3] allows the strength reduction factor for a base-isolated superstructure to be 0.375 times the one for a corresponding fixed-base structure and no larger than 2. Given that the large majority of ASCE 7 overstrength factors are between 2 and 3, the superstructure is very likely to remain elastic for the design-level seismic hazard. However, it is still possible for these structures to enter the inelastic range due to an extreme seismic demand or unexpectedly low as-built overstrength.

Constantinou and Quarshie [4], Ordonez et al. [5], Kikuchi et al. [6], Thiravechyan et al. [7] and Cardone et al. [8] investigated the response of inelastic seismically isolated structures and agreed that allowing base-isolated superstructures to yield requires careful consideration because of possible occurrence of large ductility demands. Vassiliou et al. [9-11] concluded that designing typical seismically isolated structures to behave elastically, as prescribed by current seismic design codes, is not overly conservative but a necessity that emerges from the fundamental dynamics of such structures.

This study aims at quantifying the probability that an isolated superstructure designed according to the current design codes enters the inelastic behavior range. Additionally, incremental dynamic analysis [12] is performed to determine the behavior of the isolated structure for ground motions caused by events of higher seismic hazard than the design hazard level. Huang et al [13] have presented fragility curves for the estimation of the probability of failure of base-isolated nuclear power plants for a range of spectral acceleration values. Han et al [14] used the damped spectral acceleration at the effective period of the isolators $S_a\ (T_{eff})$ as an intensity measure to determine similar fragility curves for non-ductile reinforce concrete buildings.

Four assumptions are made in the study. First, the displacement and strength capacities of the isolators are assumed to be sufficient to meet any demands. Second, friction-pendulum bearings are assumed, unless explicitly stated otherwise. Third, the overstrength, i.e., the difference between the actual and the yield strength of the isolated superstructure, is not explicitly considered in the model. Fourth, the response of the dynamic model is computed in-plane to an earthquake excitation that has a single horizontal component, disregarding the coupled bi-directional horizontal and vertical response of the isolators as well as the effect of multi-directional excitation on the response of isolated superstructure.

2 DYNAMIC MODELLING

The dynamics of a base-isolated structure, following to the work of Naeim and Kelly [15], is investigated using a two-degree-of-freedom (2-DOF) in-plane model, presented in Fig. 1. The system consisting of the isolation bearings and the isolation base is defined as the isolation system. The structure above the isolation system is defined as the isolated superstructure.

Masses m_s *and* m_b represent the mass of the isolated superstructure and the mass of the base above the isolation system, respectively. The stiffness and damping are denoted as k_s, c_s, when referring to the superstructure and as k_b, c_b when referring to the base. The stiffness k_b is the post-yielding stiffness of the isolators [16], whereas the equivalent stiffness shown in Fig. 1 is the effective stiffness k_{eff} of the isolators.

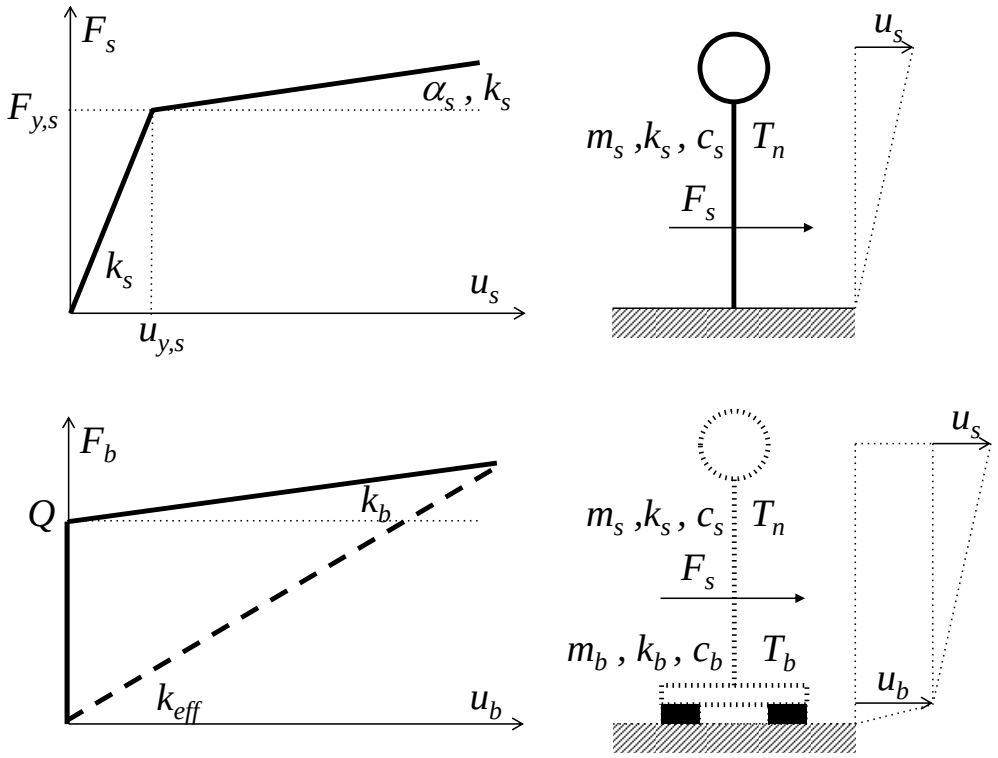

Figure 1: Parameters of the SDOF model of a fixed-base structure and of a 2-DOF model of a base-isolated structure.

Horizontal displacement u_s is the relative displacement of the superstructure with respect to the base and u_b is the horizontal displacement of the isolation bearings with respect to the ground. The ground displacement to which the system is subjected is denoted as u_g. The notation used to describe the inelastic response of fixed-base single-degree-of-freedom (SDOF) structures is adopted as follows. The vibration period of the SDOF system is T_n. The displacement ductility ratio μ is defined as:

$$\mu = \frac{u_m}{u_y} \tag{1}$$

where u_m and u_y denote the maximum inelastic displacement and the yield displacement of the SDOF system, respectively. The strength reduction factor R_y is the ratio of the minimum strength required to maintain the SDOF system response in the elastic range, $F_{el,s}$ to the SDOF system yield strength $F_{y,s}$:

$$R_y = \frac{F_{el,s}}{F_{y,s}} \tag{2}$$

The following quantities are defined for the 2-DOF model of the base-isolated structure:

1. Period and cyclic frequency of the isolated superstructure:

$$T_n = 2\pi\sqrt{\frac{m_s}{k_s}},\ \omega_n = \sqrt{\frac{k_s}{m_s}} \tag{3}$$

2a. Isolation period and cyclic frequency:

$$T_b = 2\pi\sqrt{\frac{m_s + m_b}{k_b}},\ \omega_b = \sqrt{\frac{k_b}{m_s + m_b}} \tag{4}$$

2b. Effective isolation period and cyclic frequency:

$$T_{eff} = 2\pi\sqrt{\frac{m_s + m_b}{k_{eff}}},\ \omega_{eff} = \sqrt{\frac{k_{eff}}{m_s + m_b}} \tag{5}$$

3. Non-hysteretic structural and isolation system damping ratios:

$$\xi_s = \frac{c_s}{2m_s\omega_s}, \qquad \xi_b = \frac{c_b}{2\left(m_s + m_b\right)\omega_b} \tag{6}$$

4. Mass ratio:

$$\gamma_m = \frac{m_s}{m_s + m_b} \tag{7}$$

The strength of the isolation system is defined as Q (force at zero displacement).

Dynamic equilibrium of the isolated superstructure and the base isolation system gives:

$$\left(m_s + m_b\right)\ddot{u}_b + m_s\ddot{u}_s + k_b u_b + Qz_b\left(t\right) + c_b\dot{u}_b\left(t\right) = -\left(m_s + m_b\right)\ddot{u}_g \tag{8}$$

Dynamic equilibrium of the isolated superstructure alone gives:

$$m_s\ddot{u}_s + m_s\ddot{u}_b + a_s k_s u_s(t) + (1-a_s)k_s u_{y,s} z_s(t) + c_s\dot{u}_s(t) = -m_s\ddot{u}_g \tag{9}$$

Consequently, Equations (8) and (9) become equations of motion of the combined structure-isolation system. Equations (10) and (11) are derived by dividing equations (8) and (9) by (m_s+m_b). The inelastic displacement demand for the isolation system and the isolated superstructure can be obtained by solving Equations (10) and (11) using Matlab [17].

$$\ddot{u}_b + \gamma_m\ddot{u}_s + \omega_b{}^2 u_b + \frac{Q}{m_s + m_b} z_b + 2\xi_b\omega_b\dot{u}_b = -\ddot{u}_g \tag{10}$$

$$\ddot{u}_s + \ddot{u}_b + 2\xi_s\omega_n\dot{u}_s(t) + a_s\omega_n^2 u_s(t) + (1-a_s)\omega_n^2 u_{y,s} z_s(t) = -\ddot{u}_g \tag{11}$$

An identical 2-DOF model was developed in OpenSees [18] to compute the inelastic displacement demand of both systems, using bilinear inelastic behavior models as the one shown in Fig. 1 for the superstructure and the isolators. This model gives identical results with the ones obtained using the Bouc-Wen models presented above in Matlab. The calculation process using Bouc-Wen models in Matlab was performed to quantify the fundamental parame-

ters of the problem. However, the results presented on this study are computed with bilinear models (Fig. 1) using OpenSees for reasons of computational efficiency.

3 CODE EVALUATION: DESIGN HAZARD LEVEL

Eurocode 8 [2] allows a maximum strength reduction factor value of 1.5 for base-isolated buildings, thus implying the development of limited inelastic behavior in the isolated superstructure for the design hazard level. A number of recorded ground motions were selected and scaled until its acceleration response spectrum matches the design spectrum, as defined in Eurocode 8 [2]. The 2-DOF structure of Fig. 1 was subjected to the scaled ground motion ensemble. Lognormal probability distributions were fit to the determined displacement ductility demand values of the structure for this ground motion ensemble. The probability that the structure enters the inelastic range, thus exceeding the values implied by the code, is determined through the statistical processing of the recorded ductility values.

3.1 Design of the isolated structure

The structure that has been investigated in this study is the National Opera of Greece, which belongs to the Stavros Niarchos Foundation (SNF) Cultural Center. This structure has been chosen as an example of inelastic design of base-isolated structures, as a strength reduction factor of 1.5 has been used for its seismic design [19]. The design spectrum for the structure (PGA=0.267g) was based on a microzonation study, conducted due to the importance of the project, and is shown in Fig. 2 below. The return period of this spectrum is 475 years, which corresponds to 10% probability of exceedance in any 50 year period.

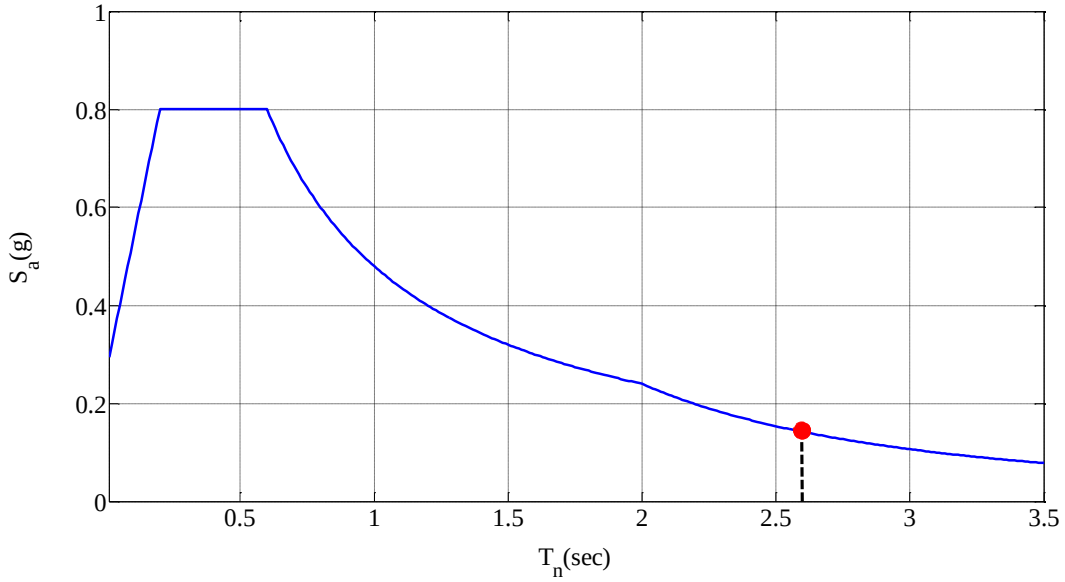

Figure 2: Elastic design acceleration spectrum [19]

The strength of the isolation system is determined using Equation (12) for friction-pendulum bearings with the coefficient of friction μ_f=0.05 (g the acceleration of gravity). The mass ratio is γ_m=0.9.

$$Q = \left(m_s + m_b\right)\mu_f g \tag{12}$$

Then, for m_s=120000 tons, Q=58860 kN. The effective period of the isolators is T_{eff}=2.6 sec. The design displacement for the isolators (ξ_{eff}=15%, S_e=0.141g) is D_d=235*1.5=351 mm. Then, the post-yielding stiffness of the isolators $k_b=(k_{eff}D_d-Q)/D_d$=303922 kN/m, which leads to a period T_b=4 sec. The yield strength of the structure for a behavior factor of q=1.5 is $F_y=(m_s+m_b)S_a(T_{eff})/q$=165536 kN.

3.2 Ground motion excitation

The ground motion ensemble used to excite the model of the isolated structure presented in Fig. 1 was taken from the strong motion database presented by Vassiliou and Makris [20]. From the 183 ground motions used that study, 20 motions were chosen for this study, using the minimization of the root-mean-squared error (*RMSE*) between the selected motions' acceleration response spectrum and the target design spectrum (Fig. 2), as performed by Carlson et al [21]. *RMSE* is defined as follows:

$$\mathrm{RMSE}=\sqrt{\frac{\sum_{i=1}^{n}\left[\ln\left(\mathrm{Sa}_{\mathrm{tar}}(\mathrm{T}_i)\right)-\ln\left(\mathrm{Sa}_{\mathrm{rec}}(\mathrm{T}_i)\right)\right]^2}{n}} \tag{13}$$

where $Sa_{tar}(T_i)$ and $Sa_{rec}(T_i)$ represent the spectral acceleration at the ith period, T_i, for the target spectrum and recorded ground motion acceleration response spectrum, respectively, and n represents the number of spectral points. The median of the selected ground motion ensemble spectra and the target spectrum are shown in Fig. 3.

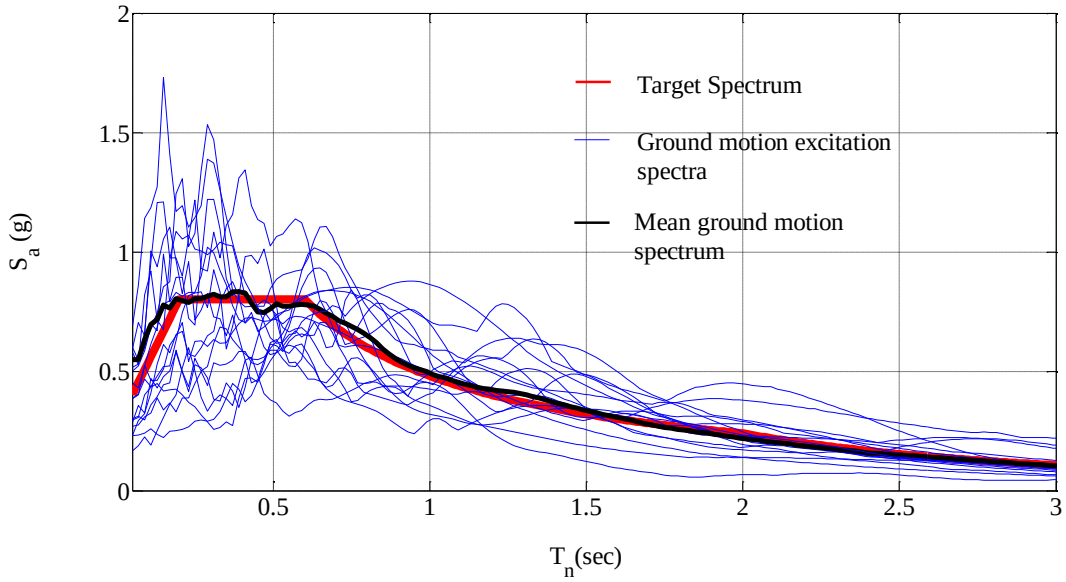

Figure 3: Elastic design acceleration spectrum (Eurocode 8) and median spectrum of the 20 ground motion excitation spectra selected based on their matching with the design spectrum (RMSE factor).

According to EC8, in the range of periods between $0.2T_1$ and $2T_1$, where T_1 is the fundamental period of the structure in the direction where the accelerogram is applied, no value of the mean 5%-damping elastic spectrum, calculated from all time histories, should be less than 90% of the corresponding value of the 5%-damping elastic response spectrum.

3.3 Probabilistic evaluation at the design hazard level

The structure presented at section 3.1 was excited by the ground motion excitation ensemble shown in Fig. 3. The displacement ductility demand developed in the superstructure was calculated for each ground motion excitation and it is shown in Fig. 4. A lognormal probability distribution was fit to the displacement ductility data and is presented in Fig. 4. The probability of exceedance of μ=1 for the given hazard level (Return period: 475 years, Probability of exceedance=10% in 50 years) is given by the PEER probabilistic PBEE evaluation methodology shown in Equation (14) [22, 23]:

$$G(EDP) = \int_0^\infty G(EDP \mid IM) f(IM) dIM \tag{14}$$

where *f(IM)* is the Probability Distribution Function (PDF) of the Intensity Measure *IM* and *G(EDP|IM)* is the Probability Distribution Function (PDF) of the Engineering Demand Parameter *EDP* given the Intensity Measure *IM*. The *EDP* chosen in this study is the displacement ductility μ and the IM is the 5% damped spectral acceleration at the effective period of the isolators S_a (T_{eff}) [14].

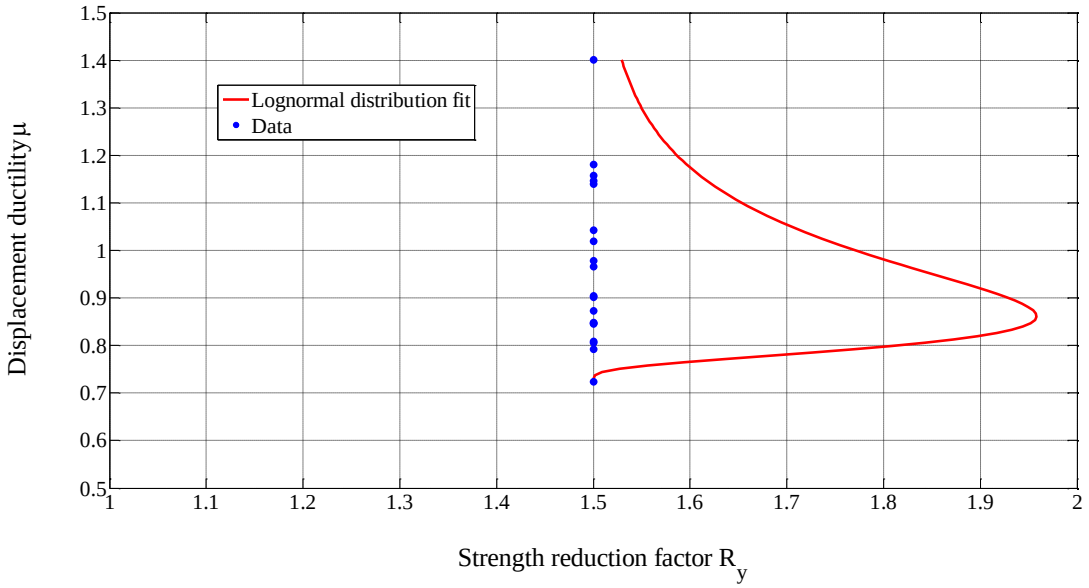

Figure 4: Displacement ductility values μ for Ry=1.5 and lognormal distribution fit

For this lognormal distribution (μ=0, σ=0.17), the probability of exceedance of μ=1 is 50% given the exceedance of the intensity measure S_a (2.59 sec)=0.141 g. The probability of the exceedance of the intensity measure S_a (2.59 sec)=0.141 g is 10% in 50 years, which corresponds to the design hazard return period of 475 years. Then, from Equation (14), the total probability that the displacement ductility μ exceeds 1 is 5%. This probability that is associated with damage in the superstructure is considered relatively high for the importance of this structure. Therefore, the choice of a strength reduction factor R_y=1.5 does not guarantee the quasi-elastic behavior implied by the code for this structure. However, the consideration of overstrength that has not been taken into account in this case study may change this conclusion, as it would reduce the probability of inelastic behavior in the superstructure.

4 CODE EVALUATION: BEYOND DESIGN HAZARD LEVEL

4.1 Incremental Dynamic Analysis

The evaluation of the existing code provisions for isolated structures for seismic hazard levels that are higher than the design hazard level requires the statistical processing of the dynamic response of the structure to a large number of strong ground motion excitations. This process can be effectively performed for the targeted hazard levels using Incremental Dynamic Analysis (IDA) [12]. The incremental analysis was performed for the fixed-base period of the isolated superstructure T_n=0.31 sec. The results of the analysis for a wide range of intensity measures S_a (T_{eff}) are shown in Fig. 5.

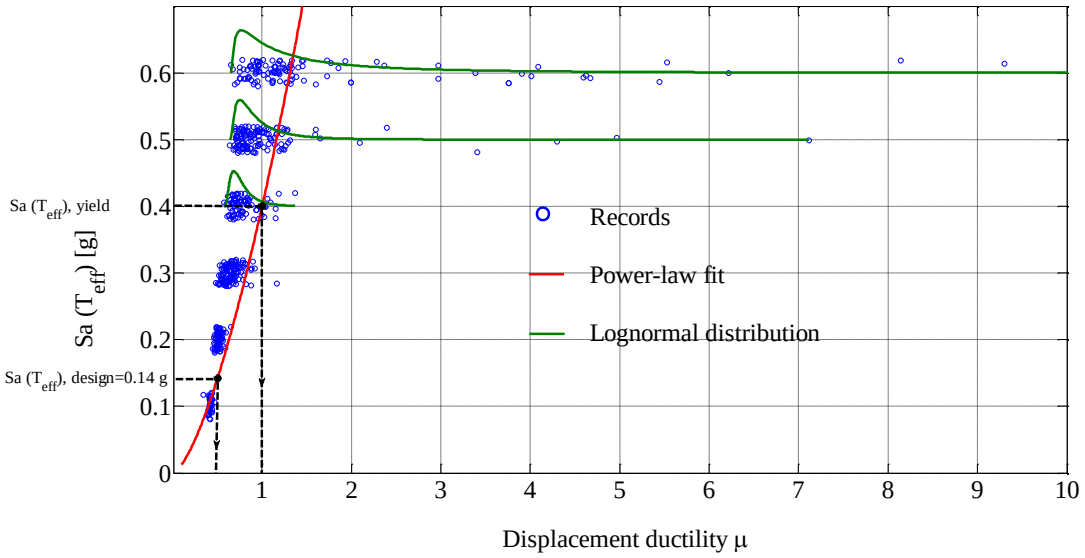

Figure 5: Displacement ductility values μ for different values of spectral acceleration $S_a(T_{eff})$, power-law fit to the presented displacement ductility values and lognormal distribution fit for each spectral acceleration $S_a(T_{eff})$

The $S_a(T_{eff})$ values presented are selected from the set {0.1g, 0.2g, 0.3g, 0.4g, 0.5g, 0.6g} within a 5% tolerance range. A power-law fit was performed to indicate the general trend of the displacement ductility μ results for varying $S_a(T_{eff})$ values. Lognormal probability distributions were fit to displacement ductility μ data for each spectral acceleration value $S_a(T_{eff})$ above the yield limit $S_a(T_{eff}),_{yield}$. According to the results of the power-law fit, the design acceleration of the structure corresponds to a displacement ductility μ=0.5. The yield spectral acceleration value, which corresponds to displacement ductility μ=1 is $S_a(T_{eff}),_{yield}$=0.4 g. This spectral acceleration, which can lead to damage in the superstructure, exceeds the design value by a factor of 3. If higher $S_a(T_{eff})$ values than this value are considered (e.g. $S_a(T_{eff})$=0.5 g or $S_a(T_{eff})$=0.6 g), extensive damage may occur in the superstructure, as the corresponding ductility demand values may exceed μ=7.

This exceedance of the design spectrum even by a factor as high as 3 over a large range of periods has been reported in numerous seismic events (Mexico City 1985, Kobe 1995, Nepal 2015) in the past. A large number of ground motions recorded on "soft" soils have produced response spectra of a sharp rather than flat shape, with well-defined peaks around the site fundamental period, as presented by Gazetas et al [24]. Thus, such high demands on isolated structures cannot be excluded from consideration.

5 CONCLUSIONS

- Two different ground motion selection procedures have been used in this study to evaluate the inelastic behavior of the National Opera of Greece for different seismic hazard levels.
- The results obtained through a spectral matching procedure based on the RMSE factor [21] indicate a 5% probability of inelastic behavior and associated damage in the superstructure for the design seismic hazard level (return period of 475 years).
- However, the results obtained through IDA [12] show that the design spectrum must be exceeded 3 times for a development of inelastic behavior in the superstructure. This scaling process was performed for selected values of spectral acceleration $S_a(T_{eff})$, which restricts the ground motion variability, compared to the spectral matching procedure that was used for the design hazard level evaluation.
- The overstrength of the superstructure was not considered in this study. The consideration of overstrength is expected to reduce the probability of inelastic behavior in the superstructure.

REFERENCES

[1] M. Higashino, S. Okamoto, Response Control and Seismic Isolation of Buildings. Taylor & Francis: London; 193–202, 2006

[2] CEN, Eurocode 8, Design of structures for earthquake Resistance—Part 1: general rules, seismic actions and rules for buildings. EN 1998-1:2004. Comité Européen de Normalisation,

[3] Structural Engineering Institute, Minimum design loads for buildings and other structures, ASCE; **7**(5), 2010

[4] M.C. Constantinou, J.K Quarshie, Response modification factors for seismically isolated bridges. *Report No. MCEER-98-0014, Multidisciplinary Center for Earthquake Engineering Research*, Buffalo, NY, 1998.

[5] D. Ordonez, D. Foti, L. Bozzo, Comparative study of the inelastic response of base isolated buildings. *Earthquake Engineering and Structural Dynamics*; **32**:151–164, 2003

[6] M. Kikuchi, C.J. Black, I.D. Aiken, On the response of yielding seismically isolated structures. *Earthquake Engineering and Structural Dynamics*; **37**(5):659–679, 2008

[7] P. Thiravechyan, K. Kasai, T.A. Morgan, The effects of superstructural yielding on the seismic response of base isolated structures., *Joint Conference proceedings, 9th International Conference on Urban Earthquake Engineering / 4th Asia Conference on Earthquake Engineering, Tokyo*, Japan; 1451-1458, 2012

[8] D. Cardone, A. Flora, G. Gesualdi, Inelastic response of RC frame buildings with seismic isolation. *Earthquake Engineering and Structural Dynamics*; **42**:871–889, 2013

[9] A. Tsiavos, M.F. Vassiliou, K.R Mackie and B. Stojadinovic, R-μ-T relationships for seismically isolated structures, *COMPDYN 2013, 4th International Conference on*

Computational Methods in Structural Dynamics and Earthquake Engineering, Kos Island, Greece, 12-14 June, 2013.

[10] A. Tsiavos, M.F Vassiliou, K.R Mackie and B. Stojadinovic, Comparison of the inelastic response of base-isolated structures to near-fault and far-fault ground motions, *VEESD 2013, Vienna Congress on Recent Advances in Earthquake Engineering and Structural Dynamics & D-A-CH Tagung*, Vienna, Austria, 28-30 August, 2013.

[11] M.F. Vassiliou, A. Tsiavos and B. Stojadinovic, Dynamics of Inelastic Base Isolated Structures Subjected to Analytical Pulse Ground Motions, *Earthquake Engineering and Structural Dynamics*, **42** (14), 2043-2060, 2013.

[12] J.D. Vamvatsikos, C.A. Cornell, Incremental Dynamic Analysis, *Earthquake Engineering and Structural Dynamics*, **31**(3): 491–514, 2002.

[13] Y-N. Huang, A.S. Whittaker, N. Luco, Seismic performance assessment of base-isolated safety-related nuclear structures, *Earthquake Engineering and Structural Dynamics*, **39**:1421–1442, 2010.

[14] R. Han, Y. Li, J.V.D. Lindt, Seismic risk of base isolated non-ductile reinforced concrete buildings considering uncertainties and mainshock–aftershock sequences. *Structural Safety*; **50**:39–56, 2014.

[15] F. Naeim, J.M. Kelly, Design of Seismic Isolated Structures: From Theory to Practice, Wiley, New York, 1999.

[16] N. Makris, G. Kampas, The engineering merit of the "effective period" of bilinear isolation systems. *Earthquakes and Structures*, **4** (4), 397-428, 2013.

[17] MATLAB and Statistics Toolbox Release 2012b, The Mathworks, Inc., Natick, Massachusetts, United States.

[18] OpenSees command language manual, S Mazzoni, F McKenna, MH Scott, GL Fenves, Pacific Earthquake Engineering Research (PEER) Center, 2006.

[19] C. Giarlelis, J. Keen, E. Lambrinou, V. Martin, G. Poulios, Dynamic behavior of the seismically isolated SNF Cultural Center in Athens, 14th World Conference on Seismic Isolation, Energy Dissipation and Active Vibration Control of San Diego, USA, 2015

[20] M.F. Vassiliou, N. Makris, Estimating Time Scales and Length Scales in Pulselike Earthquake Acceleration Records with Wavelet Analysis, *Bulletin of the Seismological Society of America*, vol. 101, no. 2, pp. 596-618, 2011

[21] C. Carlson, D. Zekkos, and A. Athanasopoulos-Zekkos, Predictive Equations to Quantify the Impact of Spectral Matching on Ground Motion Characteristics. *Earthquake Spectra*, 2015

[22] S. K. Kunnath, Application of the PEER PBEE Methodology to the I-880 Viaduct. *PEER Report 2006/10*. Pacific Earthquake Engineering Research Center, College of Engineering, University of California, Berkeley, February 2007

[23] K. R. Mackie, J. M. Wong, B. Stojadinovic, Integrated Probabilistic Performance-Based Evaluation of Benchmark Reinforced Concrete Bridges, *PEER Report 2007/09.* Pacific Earthquake Engineering Research Center, College of Engineering, University of California, Berkeley, January 2008

[24] G. Gazetas, A. Ziotopoulou, Bi-normalized Response Spectrum for a Rational Soil-Structure Interaction Analysis, Workshop on Soil Structure Interaction (SSI) Knowledge and Effect on the Seismic Assessment of NPPS Structures and Components, Otawa, Canada, 6-8, 2010